Available online at www.sciencedirect.com
ScienceDirect
Journal of Power Sources 164 (2007) 33–41
JOURNAL OF POWER SOURCES
www.elsevier.com/locate/jpowsour

Fabrication and impedance studies of DMFC anode incorporated with CNT-supported high-metal-content electrocatalyst

King-Tsai Jeng *, Chun-Ching Chien, Ning-Yih Hsu, Wan-Min Huang, Shean-Du Chiou, Su-Hsine Lin

Institute of Nuclear Energy Research (INER), P.O. Box 3-19, 1000 Wenhua Road, Longtan, Taoyuan 32546, Taiwan

Received 8 August 2006; received in revised form 28 September 2006; accepted 29 September 2006
Available online 13 November 2006

Abstract

In this study, the fabrication of a direct methanol fuel cell (DMFC) anode with the incorporation of a multiwalled carbon nanotube (CNT)-supported high-metal-content Pt/Ru electrocatalyst, i.e., 40 wt%Pt-20 wt%Ru/CNT, using a novel approach and the resultant DMFC performances were investigated. Employing a vacuum filtration method, we were able to successfully fabricate the DMFC anode with a good electrode structure using an in-house prepared Pt-Ru/CNT electrocatalyst. The catalyst layer was formed directly on a Teflon-treated carbon cloth having a buckypaper texture with a catalyst loading of 4.0 mg cm^{-2}. From single-cell tests, excellent cell performances were obtained. At 80 °C, the power density was found to be as high as >100 mW cm^{-2}. This can be attributed to a thinner catalyst layer formed with a more efficient utilization of the catalyst than that using a low-metal-content counterpart, i.e., 20 wt%Pt-10 wt%Ru/CNT, as reported in an earlier study. However, the Nafion® ionomer content in the catalyst layer played a key role in the anode fabrication to obtain a good cell performance. In addition, the electrochemical impedance spectroscopy (EIS) with a constant phase element (CPE)-based equivalent-circuit model was employed to analyze the fabricated anode. It distinctively revealed some specific characteristics in the resistances and the interface properties. Overall, the obtained impedance results are somewhat different from those of a conventional DMFC anode with the catalyst layer coated onto a porous gas diffusion layer (GDL) on a carbon backing material. Based on the experimental results and the impedance analyses, the high-metal-content Pt-Ru/CNT catalyst was found to be much more favorable and suitable for use as a DMFC anode catalyst.

Keywords: Direct methanol fuel cell; Dynamic hydrogen electrode; Electrochemical impedance spectroscopy; Constant phase element; Electrocatalyst; Buckypaper

1. Introduction

Although significant advances have been achieved for direct methanol fuel cell (DMFC) systems in recent years, considerable efforts are still needed to make them more commercially practical. Among them, the development of advanced electrocatalysts is of vital importance. In responding to such demands, recently a variety of carbon nanomaterials (CNMs), e.g., carbon nanosphere (CNS) [1], carbon nanofiber (CNF) [2–5], carbon nanohorn (CNH) [6], carbon nanocoil (CNC) [7,8], etc., and in particular carbon nanotube (CNT) [9–16], have been intensively investigated as a new generation of electrocatalyst supports due to their distinctive physical and chemical characteristics as well as corrosion resistances [17]. The CNF-supported Pt, for example, was reported to exhibit a structure effect that allows the operation of DMFC at low air flow rates [18]. This feature is very important with respect to the operation of small DMFCs for consumer electronics applications, because the abilities to supply air in such small equipments are severely limited.

However, unlike much denser, smaller size conductive carbon black powders, carbon nanomaterials are generally very fluffy and bulky. Thus, CNM-supported electrocatalysts are very difficult to prepare into suitable electrode structures with thin catalytic layers by any conventional means, particularly when a low-metal-content (e.g., <50 wt% metal content) catalyst is used to fabricate a high catalyst loading (e.g., 4 mg cm^{-2}) electrode. In other words, too much CNM-based carbon support in the catalyst is not favorable for the proper fabrication of a usable DMFC electrode. For instance, it is difficult to bind a CNM-supported low-metal-content catalyst well together on the

* Corresponding author. Tel.: +886 3 471 1400x5025; fax: +886 3 471 1064.
E-mail address: ktjeng@iner.gov.tw (K.-T. Jeng).

0378-7753/$ – see front matter © 2006 Elsevier B.V. All rights reserved.
doi:10.1016/j.jpowsour.2006.09.097

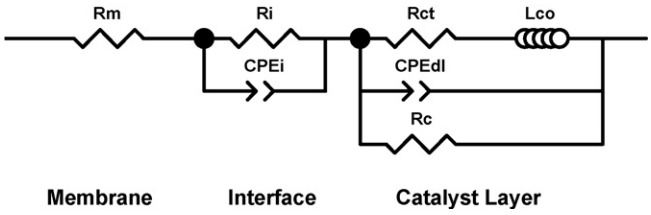

Fig. 1. The proposed CPE-based equivalent-circuit model for impedance analysis of DMFC anode.

coated electrode unless an excessive amount of Nafion® solution is employed. This, in turn, will give rise to a thick catalyst layer and high ionic resistance when the electrode is assembled into a membrane electrode assembly (MEA). Mass transfer limitation of the fuel solution is also likely to occur in the reaction process and leads to poor cell performance. Therefore, the fabrication of DMFC electrodes using CNM-supported catalysts has indeed caused a serious problem. Such difficulties are also found in the fabrication of DMFC electrodes using carbon-supported catalysts, particularly under high-catalyst-loading conditions. In this study, a novel anode fabrication approach was employed so as to solve these problems using a high-metal-content Pt-Ru/CNT anode electrocatalyst with much improved DMFC performance.

In addition, since the properties of the fabricated electrode are dependent on its materials and fabrication methods, it is of special interest as well as vital importance to investigate the electrochemical characteristics of the anode so as to improve the anode fabrication and the cell performance. Therefore, electrochemical impedance spectroscopy was used to analyze the electrochemical reaction behavior of the fabricated DMFC anode. The equivalent-circuit model used in this study is a constant phase element (CPE)-based model as described in an earlier report [19]. So far, only few studies [19,20] have involved the use of CPEs to replace ideal capacitors in the DMFC-related impedance investigations. Thus, it deserves more in-depth studies using this new approach. Although the anode is the main concern in this study, this particular model includes three closely related sections, i.e., membrane, interface and catalyst layer, in the analyses. In setting up the experimental apparatus, a small-size DMFC has to be fabricated and the cathode of the DMFC can then be readily converted into a dynamic hydrogen electrode (DHE) working as a reference. In other words, this impedance experiment device is in fact functioning as a pseudo rather than a true DMFC.

2. Impedance model

The impedance model for the DMFC anode employed in this study is a CPE-based equivalent circuit model, which takes into account the Faradaic reaction in the catalyst layer in conjunction with the contributions from both the membrane and the interface, as shown in Fig. 1. The CPEs are used in place of ideal capacitors, which are commonly found in conventional equivalent circuit models, to account for the non-uniform structure of the related electrode sections. More theoretical background on the CPE can be referred to the edited book by Barsoukov and Macdonald [21], and the detailed descriptions of this proposed model can be found in one of our previous reports [19]. In the figure, R_m denotes the resistance of the membrane and R_i represents the resistance of the interface between the membrane and the catalyst layer; R_{ct} denotes the charge transfer resistance; C_d is the double-layer capacitance; R_c represents the resistance of the solid phase in catalyst layer; L_{co} is the inductance. The inductive behavior means that the current signal follows a voltage perturbation with a phase delay is due to the slowness of the relaxation of $(CO)_{ads}$ coverage.

Notably, this particular impedance model incorporates two CPEs to account for the anode-membrane interface and the catalyst layer, respectively. Hence, the complex impedance of the equivalent circuit of the interface ($Z_{Interface}$) can be expressed as,

$$Z_{Interface} = \frac{R_i}{1 + R_i Q_i (j\omega)^{p_i}} \quad (1)$$

where p_i is the adjustment parameter of the CPE and Q_i is the admittance constant at the interface. Similarly, the complex impedance of the equivalent circuit of the catalyst layer ($Z_{Catalyst\,Layer}$) can be expressed as,

$$Z_{Catalyst\,Layer} = \frac{R_c(R_{ct}^2 + \omega^2 L_{co}^2)}{1 + R_c[R_{ct} - j\omega L_{co} + Q_{dl}(j\omega)^{p_{dl}}]} \quad (2)$$

where p_{dl} is the adjustment parameter of the CPE; L_{co} is the inductance element and Q_{dl} is the admittance constant in the catalyst layer. The overall impedance is simply the summation of the specific impedance in each section.

3. Experimental

3.1. Fabrication of DMFC anode and single-cell DMFC

The procedure for the preparation of Pt-Ru/CNT anode catalyst was described elsewhere [22,23] using a modified polyol synthesis method. A multiwalled carbon nanotube (MWCNT) was employed in the catalyst synthesis so as to ensure having a good electrical conductivity for all elements of the catalyst carbon support. The targeted high-metal-content anode catalyst, i.e., 40 wt%Pt-20 wt%Ru/CNT, was prepared in-house. Then, the prepared anode catalyst was fabricated into a DMFC anode having a loading of 4.0 mg cm^{-2} (metal basis). Briefly, a known amount of the electrocatalyst was first well-mixed with a designated amount (e.g., 20–70 wt% dry basis) of a Nafion® solution (containing 10 wt% Nafion® ionomer), together with suitable amounts of isopropanol and deionized water, and then applied to one side of a Teflon-treated carbon cloth (ElectroChem, Inc., model: EC-CC1-060T) by vacuum filtration followed by a physical leveling procedure. The filtration setup used was a ceramic funnel connected to a vacuum suction device. In the operation, a piece of Teflon-treated, or wet-proofed, carbon cloth substrate was employed as a filtration medium and the catalyst/Nafion® solution mixture was filtrated through the filter funnel several times until the filtrate became clear. Then, the coated catalyst layer was further leveled evenly on the carbon cloth using a

spatula followed by a cold-press procedure at 0.30 kN cm^{-2} for 10 min with the electrode wrapped in a PVC film. Thereafter, the electrode was dried in air for several days before being cut and hot pressed into an MEA.

A commercial gas diffusion electrode (GDE) with a platinum black loading of 4.0 mg cm^{-2}, obtained from E-TEK, was employed as the base cathode. The electrode dimension was 1.5 cm × 1.5 cm. In the preparation of MEA, the prepared anode and the GDE cathode were hot-pressed onto each side of a Nafion® 117 membrane, respectively, at 135 °C under an applied pressure of 0.75 kN cm^{-2} for 5 min. Then, the MEA was fabricated into a single-cell DMFC using two graphite current collectors (engraved with flow fields on one side) together with two gold-coated stainless steel end plates and fasten with bolts and nuts. The gaskets were made of silicon rubber.

3.2. Investigation on DMFC performance

The single-cell DMFC was first activated at 40 °C and 0.2 V for 4 h by feeding air to the cathode and 1 M methanol solution to the anode, and then continued to activate at 60 and 80 °C for 4 h each. After completion of the activation process, it was tested between 40 and 80 °C for several days by feeding 1 M methanol solution (40 mL min^{-1}) with circulation through the anode compartment, and by flowing air (0.2 L min^{-1}, 20 psi back pressure) through the cathode compartment. Performance tests of the DMFC were conducted using a fuel cell test station developed by APFCT. The cell performance curves, i.e., plots of cell voltage (V) versus current density (I) and power density (P) versus current density (I), were collected and compared.

3.3. Electrochemical impedance investigation on DMFC anode

The electrochemical impedance experiments were undertaken over a range of potential from 0.3 to 0.6 V (DHE) using the same procedure and a similar setup as described elsewhere in an earlier report [19]. Briefly, a small single-cell DMFC was fabricated and the cathode was ingenuously converted into a dynamic hydrogen electrode (DHE) as a reference during the experiments. The investigated potential range was chosen to match the general functioning of a DMFC under normal operation conditions. In conducting the experiments, the frequency generator/analyzer used was a Solartron SI 1260 Impedance Spectroscope controlled by a personal computer and coupled to a potentiostat (Solartron 1286) to support the modulation of large dc currents. The amplitude of the sinusoidal potential signal was 10 mV. The experimental data were collected between 5 mHz and 10 kHz frequencies and the electrochemical impedance spectra were obtained accordingly. The value of the parameter of each electrical circuit element was determined from the experimental data using the Z-View software (Scribner Associates).

The simulation modeling procedure and method are detailed in the operation manual of the Z-View Software. Briefly, after collecting the experimental data, the models to be simulated are defined forming various equivalent circuits. Various elements can be employed in the equivalent circuits. The initial estimates for all elements are entered and the element values to be calculated are selected. Then, the simulation is performed based on an instant-fit approach by calculating the minimal deviation through a root-mean-square method. The modeling simulations were carried out between 5 mHz and 10 kHz. All of the errors of the modeling parameters were kept within 1% in this study.

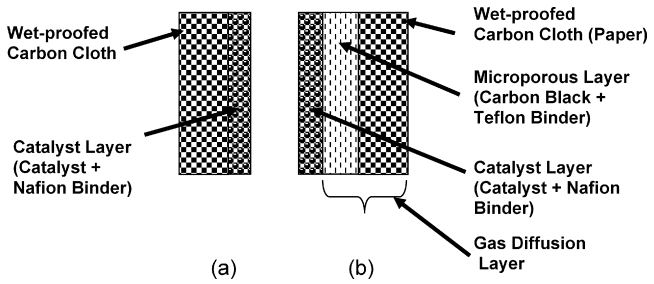

Fig. 2. Electrode structure of (a) this study, and (b) a conventional design.

4. Results and discussion

4.1. On fabrication of DMFC anode using high-metal-content Pt-Ru/CNT catalyst

Overall, the in-house prepared high-metal-content anode catalyst, i.e., 40 wt%Pt-20 wt%Ru/CNT, exhibited a good catalyst morphology and the desired composition. The metal deposition efficiency from the catalyst reactant solution was found to be >97%. In addition, the average particle size for the catalyst was about 3.7 nm and the atomic ratio of Pt:Ru was 1:0.988.

The fabrication of anode in this study using a CNT-supported high-metal-content Pt-Ru catalyst was conducted in a way somewhat different from the conventional method as shown in Fig. 2. It can be seen that the approach used in this study directly coated the catalyst layer on a Teflon-coated carbon cloth substrate while the conventional method incorporated a porous gas diffusion layer (GDL) produced by a layer of Teflon-bonded carbon powder. In fact, this gas diffusion layer generally has a very compact and tight structure not suitable for applying the filtration operation. In addition, the elimination of such a tight porous GDL layer was helpful in reducing some of the electrode resistances.

On the other hand, the Teflon-coated carbon cloth in fact also served as a more porous GDL. The in-house prepared CNT-supported Pu-Ru catalyst is illustrated in Fig. 3(a). After conducting the vacuum filtration, it can be seen that the catalyst layer on the anode formed a carbon nanotube paper or "buckypaper" type structure [24,25] with the carbon nanotubes tangled together in bundles and oriented randomly forming a rather porous structure as shown in Fig. 3(b). In addition to the physical functioning among the CNT elements, the Nafion® solution acted as an active binder to hold the CNT-supported catalyst more tightly. It is envisioned that this highly porous buckypaper-type structure is able to maintain the good ionic and electrical conductivities of the catalyst layer and indeed should also be very favorable for the transport of the DMFC

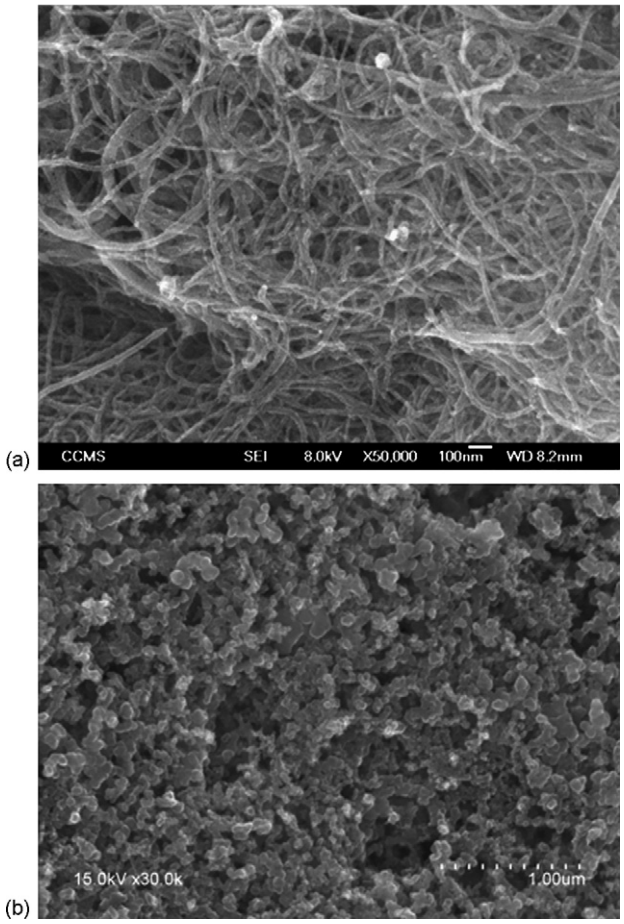

Fig. 3. SEM images of (a) an in-house prepared high-metal-content Pt-Ru/CNT, and (b) a porous catalyst layer with a buckypaper texture on the anode using a vacuum filtration approach.

fuel solution. However, it should be pointed out that the resultant anode texture was strongly dependent on the amount of Nafion® solution used in the fabrication process. If too little Nafion® solution was used as a catalyst binder, the catalyst layer was loose. The result was that it cracked and exfoliated easily. On the other hand, if too much Nafion® solution was applied, the catalyst layer became too thick although the binding condition of the catalyst was better. Under such conditions, it also cracked to some extents when dried. Although the use of a hot-press procedure for making the MEA can alleviate these problems to some extents, still only a suitable amount of the Nafion® solution should be used in the anode catalyst layer fabrication.

In this study, it was found that an electrode base with a diameter of 9.5 cm (70.85 cm^2 in total area) should have about 10 ml of 10 wt% Nafion® solution for coating the high-metal-content catalyst to obtain an optimal catalyst layer condition. Assuming the density of the Nafion® solution is 0.78, the catalyst layer coating is equivalent to having about 62.3 wt% of the dried Nafion® ionomer in the catalyst layer. The cell voltages of the DMFC measured at 300 mA cm^{-2} using different anodes fabricated with various Nafion® ionomer contents are compared and shown in Table 1. It is well-known that the Nafion® content has a significant impact on the utilization of the catalyst and the transport of the ionic species in the catalyst layer, which strongly affects the cell performance. In fact, in this study there was a combined effect of several factors, e.g., Nafion® content, catalyst layer thickness, catalyst binding condition, catalyst layer structure, etc., on the cell performance. These factors are closely interrelated and should be properly balanced in order to achieve the best result.

Using a combinatorial approach, the most active composition of a Pt-Ru-Nafion® electrocatalyst for the electrooxidation of methanol was reported [26] to have 36.4% of the dried Nafion® ionomer and 63.6% of the catalyst, just opposite to our finding, which did not use any carbon powder support for the catalyst. This illustrated the pronounced effect of the carbon content, or the catalyst metal content, on the catalyst layer fabrication involving the use of a Nafion® solution. The thickness of the catalyst layer of this particular study was found to be about 120–150 μm, which was considered to be very thick for a membrane fuel cell electrode. This was attributed mainly to the bulky size of the used CNT (∼1–2 μm in length) and its strong tendency to tangle together as well as a high catalyst loading at 4 mg Pt-Ru cm^{-2}. However, the catalyst layer appeared to be much more compact and smoother than that using a low-metal-content catalyst, i.e., 20 wt%Pt-10 wt%Ru/CNT, in an earlier study [23]. In general, the anode coated with the low-metal-content catalyst required twice as much of Nafion® solution to make a decent anode and the resultant anode catalyst layer was twice in thickness as well.

Nevertheless, one of the unique advantages for this particular catalyst application approach is that it ensures the applied catalyst is totally loaded onto the electrode surface due to the use of a repeated filtration operation until the filtrate is clear. The catalyst can be evenly distributed and the catalyst loading can be properly controlled at the electrode fabrication stage. On other hand, the conventional methods, such as brushing, printing and spraying, generally have significant amounts of catalyst ink residuals left on brushes, spraying guns, printing screens, bottles or beaker, giving rise to severe errors in this respect. This drawback is especially pronounced when a small amount of catalyst is involved in the electrode preparation process.

Table 1
Cell voltage of DMFC measured at 300 mA cm^{-2} using different anodes fabricated with 40 wt%Pt-20 wt%Ru/CNT and various Nafion® ionomer contents at a catalyst loading of 4.0 mg cm^{-2} (catalyst metal basis)

Ionomer content (wt%)[a]	24.8	39.8	49.8	56.9	62.3	66.6	69.8
Cell voltage (V)	0.114	0.201	0.275	0.307	0.324	0.315	0.297

Operating conditions: MeOH (1 M, 40 mL min^{-1}), air (0.2 L min^{-1}).
[a] Ionomer content (wt%) = wt. of dry ionomer × 100/(wt. of dry ionomer + wt. of Pt-Ru/CNT).

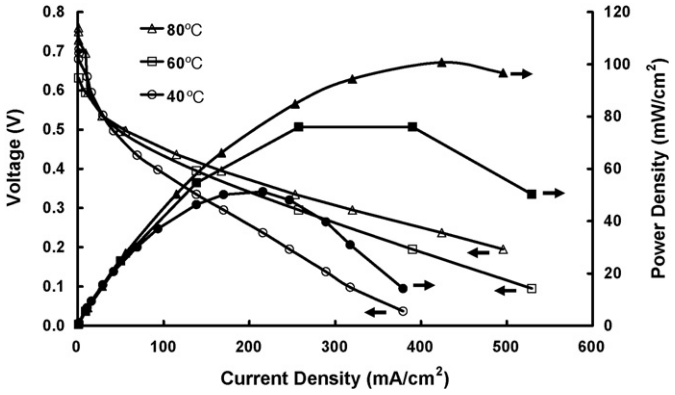

Fig. 4. The performances of the fabricated single-cell DMFC at various operating temperatures using a 40 wt%Pt-20 wt%Ru/CNT anode electrocatalyst coupled with a commercial Pt black-based cathode (E-TEK). Operating conditions: MeOH (1 M, 40 mL min^{-1}), air (0.2 L min^{-1}).

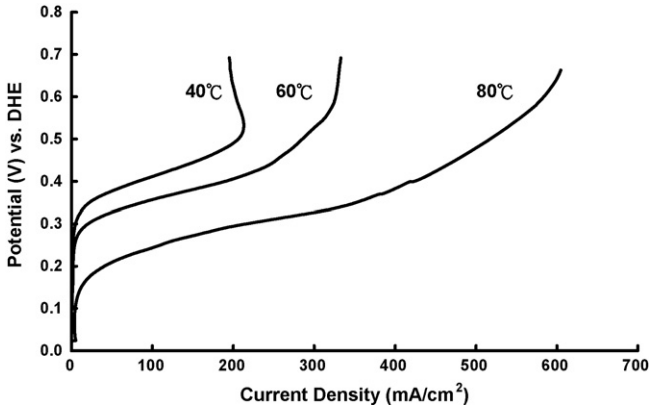

Fig. 5. The polarization curves of the DMFC anode (vs. DHE) obtained at various temperatures when operated with 1 M CH_3OH and at ambient pressure. The ohmic drop was corrected.

4.2. Performance of single-cell DMFC incorporated with high-metal-content Pt-Ru/CNT anode catalyst

At the beginning, the performance of the single-cell DMFC was found to be time-dependent. In fact, after the activation stage, it surprisingly took 3–4 days with an 8 h day^{-1} operation to reach a steady condition in the cell performance. This was indicative of a thick catalyst layer that it takes a much longer time than expected to get into an effectively operational condition. Under a steady state condition, the performances of the fabricated single-cell DMFC at various temperatures are illustrated in Fig. 4. As the temperature increases, the effective diffusion coefficient of methanol in the Nafion® membrane increases. This causes an increase in the methanol crossover and, in turn, a lowering of the cathode potential. Therefore, the cell exhibited a little higher in performance with 40 °C than with 60 °C at the very low current density region, including the OCV. Clearly, the fabricated cell using prepared anode incorporated with a higher metal-content catalyst, i.e., 40 wt%Pt-20 wt%Ru/CNT, significantly outperformed the comparison counterpart using a lower metal-content catalyst, i.e., 20 wt%Pt-10 wt%Ru/CNT, anode at the same catalyst loading as shown in a previous study [23]. A maximum power density of 100.3 mW cm^{-2} was obtained around 0.23 V with a current density of 436 mA cm^{-2}.

This improved performance can be attributed to several factors, including (i) the anode with high-metal-content Pt-Ru/CNT electrocatalyst was well-bonded that enhances its electrical conductivity and electrocatalytic activity, (ii) the anode incorporated with a high-metal-content Pt-Ru/CNT electrocatalyst had a thinner catalyst layer and a smaller ionic resistance, and (iii) the porous buckypaper-type structure of the catalyst layer resulted in a sufficient supply of fuel and a highly utilization of the high-metal-content Pt-Ru/CNT electrocatalyst at the anode. It is anticipated, however, that the catalyst loading of DMFC can be significantly reduced in the near future through the use of an anode catalyst with an even higher catalyst metal content. For instance, using a 50 wt%Pt-25 wt%Ru/CNT anode catalyst, it is estimated that both the amount of the Nafion® solution required and the thickness of the catalyst layer formed can be reduced to about 50% those of this study. Therefore, substantial improvements in the cell performance are expected. In fact, some of our preliminary experiments have already showed such very positive effects. Of course, the use of a very high-metal-content CNT-supported catalyst is still subject to the severe constraints of good catalyst morphology and composition.

4.3. On electrochemical impedance of DMFC anode incorporated with high-metal-content Pt-Ru/CNT catalyst

The polarization curves of the DMFC anode at various temperatures are shown in Fig. 5. It is obvious that these curves are temperature-dependent with the higher the temperature the stronger the anodic reaction. The potential range between 0.3 V (DHE) and 0.6 V (DHE) is roughly corresponding to the region in a normal DMFC operation that we are interested in. From the impedance spectroscopic investigation using a CPE-based equivalent-circuit model in conjunction with the considerations of both membrane and interface on the DMFC anode, the resultant Nyquist plots at various temperatures are illustrated in Figs. 6–8 while the corresponding Bode plots are shown in Figs. 9–11. Those marked points are the experimental data while the solid lines are the fitting curves of the CPE-based model. It can be seen that, experimentally and theoretically, all are in

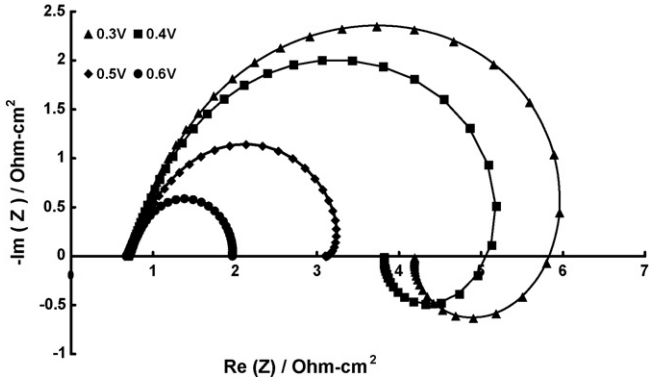

Fig. 6. The Nyquist plots of the DMFC anode at various potentials (vs. DHE) obtained at frequencies between 10 kHz and 5 mHz and 40 °C.

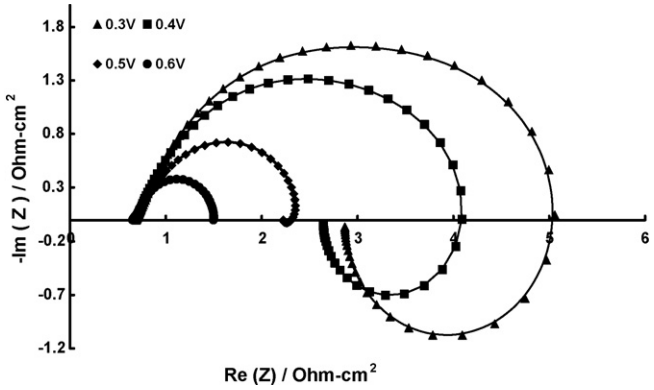

Fig. 7. The Nyquist plots of the DMFC anode at various potentials (vs. DHE) obtained at frequencies between 10 kHz and 5 mHz and 60 °C.

good fitting conditions. The corresponding fitting parameters are listed in Tables 2–4. In general, these Nyquist plots are very similar in shapes with slightly distorted, inverted semicircles. The inductance effects at low potentials (i.e., 0.3 and 0.4 V DHE^{-1}) are clearly observed with the existences of reversed semicircles in the Nyquist plots. They are potential-dependent as well as temperature-dependent. With a higher potential, the anodic reaction became more active and complete. As results, all the resistance and the inductance parameters naturally became smaller in values.

However, it should be noted that when a low-metal-content anode catalyst, i.e., 20 wt%Pt-10 wt%Ru/CNT, was used, it generally could not obtain such well-defined Nyquist plots and no semicircles could be found. This might be caused mainly by a loose structure of the thick catalyst layer in the fabricated anode. In addition to a loose electrode structure of the thick catalyst layer, the use of a CNT-supported low-metal-content anode catalyst also gives rise to poor catalyst utilization, high electrode resistance and poor cell performance. Therefore, the characteristics of Nyquist plots are totally different.

By careful examinations of the impedance plots, however, distinctive differences can be found compared to those reported in an earlier study with a conventional anode design and a commonly used anode nanocatalyst Pt-Ru/C [19]. Notably, in this study the anode did not strongly exhibit its interface character-

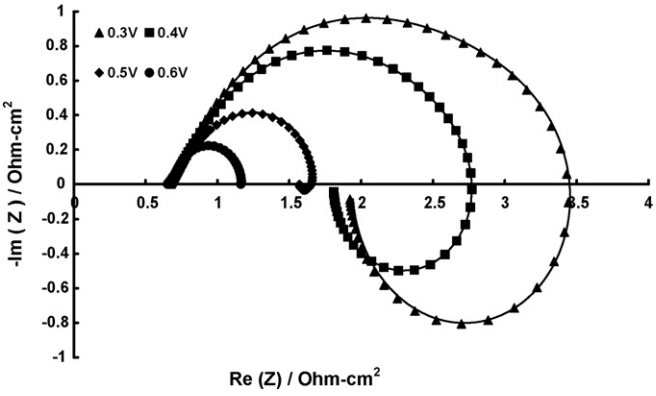

Fig. 8. The Nyquist plots of the DMFC anode at various potentials (vs. DHE) obtained at frequencies between 10 kHz and 5 mHz and 80 °C.

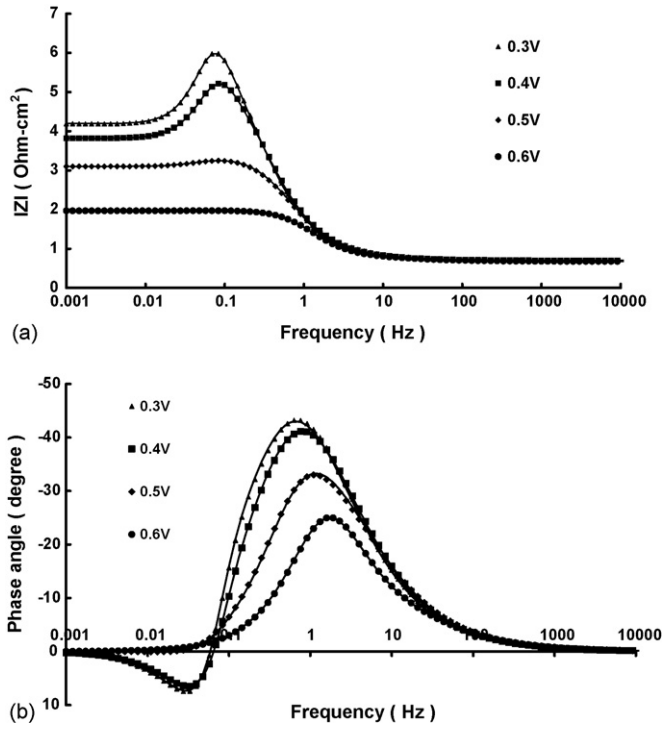

Fig. 9. The Bode plots of the DMFC anode at various potentials (vs. DHE) and 40 °C: (a) resistance magnitude against frequency and (b) phase angle against frequency.

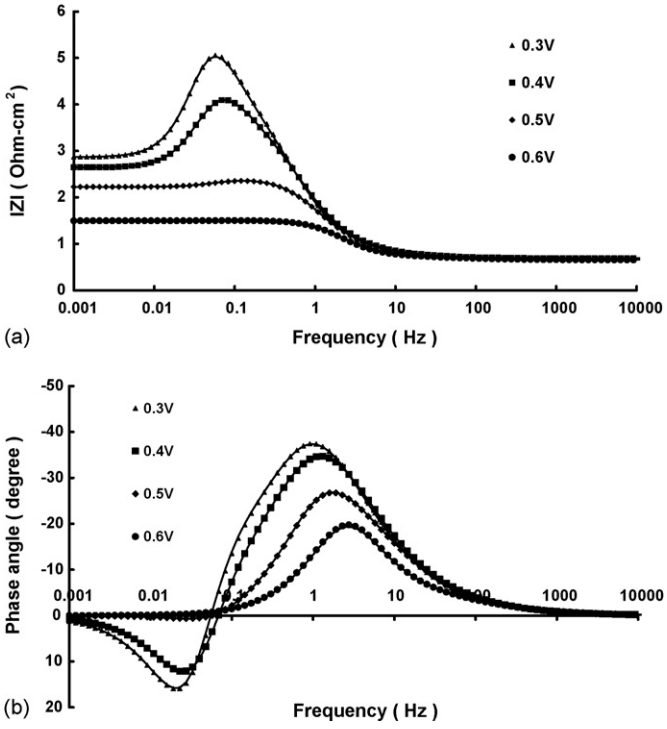

Fig. 10. The Bode plots of the DMFC anode at various potentials (vs. DHE) and 60 °C: (a) resistance magnitude against frequency and (b) phase angle against frequency.

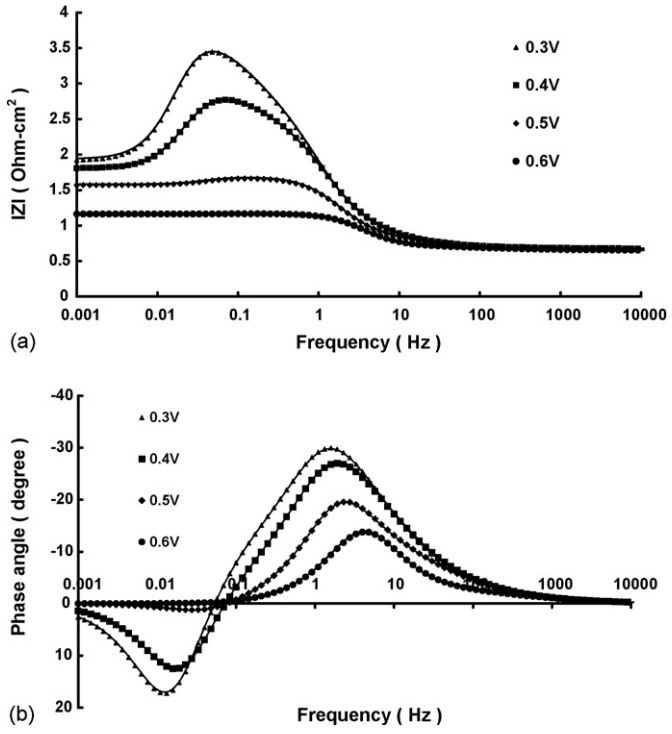

Fig. 11. The Bode plots of the DMFC anode at various potentials (vs. DHE) and 80 °C: (a) resistance magnitude against frequency and (b) phase angle against frequency.

istics as judged from the respective Nyquist plot which exhibits no apparent flattening-shape at the related region. The CPEs at the interface approaching to that of the ideal capacitors are evidenced by the adjustment parameters closing to 1.0 as listed in the tables. This indicated the formation of a compact and stable interface thin layer from the anode fabrication. In addition to these particular features, the resistance of the anode was found to be much smaller than that found in the previous study. This can be attributed to the elimination of a porous gas diffusion layer in the anode fabrication, which tends to reduce some resistances of the anode. If the effects of the roughness of the catalytic layer and the non-uniform distribution of the catalyst are considered, then the impedance of the Pt-Ru/CNT anode typically exhibiting a somewhat non-semicircular response in the Nyquist plot is very natural. Although the interface was less a pronounced feature compared to that in the previous study, overall the model gave excellent fittings. In fact, this could be a good sign. The disappearance of an interface feature means the electrochemical reaction directly occurs at the bulk catalyst layer and the resultant resistance can be lower as reflected in the Nyquist plots.

The impedance analyses based on the use of the Bode plots are also very interesting and useful. At the two extremes of the frequency range in the resistance versus frequency plot, the values of the two resistances can be simplified to:

$$f \to 0 \quad |Z| \to R_m + R_i + \frac{R_c R_{ct}}{R_c + R_{ct}} \tag{3}$$

$$f \to \infty \quad |Z| \to R_m \tag{4}$$

However, in this study the CPE-based model is applied to a limited frequency range of 5 mHz–10 kHz to be more physically realistic [21]. At 0.3 V (DHE), a characteristic hump appears at a frequency around 0.09 Hz and gradually decreases as the controlled potential increases and eventually disappears at 0.6 V (DHE). The hump broadens and becomes more distinctive as the reaction temperature increases. The resistance flattens and approaches to the same value, i.e., R_m, in a featureless manner as the frequency increases to 10 kHz. On the other hand, in the phase angle versus frequency plot, there are two humps with one upward around >0.09 Hz and one downward (<0.09 Hz). This particular frequency is corresponding to the occurrences of the maxima of the humps in the resistance versus frequency plots. Similarly, the humps are more pronounced at a lower potential. In addition, there is a tendency for these humps to shift towards the higher frequency direction as the temperature increases. These distinctive characteristics are very useful in examining the conditions of a fabricated anode under normal operating conditions. The quality of the prepared anode catalyst as well as the fabrications of anode and MEA can be readily detected and distinguished.

From the analyses of the collected fitting parameters, it was found that the membrane resistance, R_m, is close to that of the previous study [19]. It decreased, however, as the temperature increased due to the increase in the proton mobility. This might also be caused by the swelling effects on the microscopic structures of the membrane that the ratio of the effective ionic conducting length (l_{eff}) to the effective ionic conducting area (A_{eff}) increased. On average, the R_m decreased 2–4% as the temperature increased every 20 °C. Unlike the ideal capacitive interface, the porous structure of the catalyst layer was reflected on its adjustment parameter, $CPE_{dl\text{-}P}$, which was around 0.6–0.7. The higher potential demanded more vigorous methanol oxidation reaction and, therefore, caused decreases in the inductive parameter, L_{co}, and the adjustment parameter, $CPE_{dl\text{-}P}$. More precisely, it should be noted that the oxidation reaction of methanol at the anode can be roughly separated into two steps: $CH_3OH \to CO_{(ads)} \to CO_2$, and L_{co} is an indicator of the amount of $CO_{(ads)}$ on the catalyst surfaces. As the tem-

Table 2
Fitting parameters for the CPE-based equivalent-circuit model at various potentials with the DMFC anode operating at 40 °C

Potential (V DHE^{-1})	R_m (Ω cm^2)	R_i (Ω cm^2)	$CPE_{i\text{-}Q}$ (F cm^{-2})	$CPE_{i\text{-}p}$	R_{ct} (Ω cm^2)	L_{co} (H cm^{-2})	$CPE_{dl\text{-}Q}$ (F cm^{-2})	$CPE_{dl\text{-}p}$	R_c (Ω cm^2)
0.3	0.706	1.980	0.280	0.998	1.935	2.400	0.338	0.670	7.200
0.4	0.696	1.868	0.253	1.000	1.735	2.060	0.318	0.671	4.725
0.5	0.686	1.800	0.178	0.999	1.800	1.556	0.302	0.680	0.945
0.6	0.676	1.126	0.135	1.000	1.913	1.022	0.289	0.670	0.186

Table 3
Fitting parameters for the CPE-based equivalent-circuit model at various potentials with the DMFC anode operating at 60 °C

Potential ($V\ DHE^{-1}$)	R_m ($\Omega\ cm^2$)	R_i ($\Omega\ cm^2$)	$CPE_{i\text{-}Q}$ ($F\ cm^{-2}$)	$CPE_{i\text{-}p}$	R_{ct} ($\Omega\ cm^2$)	L_{co} ($H\ cm^{-2}$)	$CPE_{dl\text{-}Q}$ ($F\ cm^{-2}$)	$CPE_{dl\text{-}p}$	R_c ($\Omega\ cm^2$)
0.3	0.691	1.287	0.252	0.989	1.103	3.600	0.321	0.650	4.680
0.4	0.682	1.214	0.227	0.973	0.989	2.472	0.302	0.651	3.071
0.5	0.672	1.170	0.160	0.992	1.026	0.778	0.287	0.660	0.614
0.6	0.662	0.732	0.121	0.991	1.090	0.511	0.275	0.650	0.121

Table 4
Fitting parameters for the CPE-based equivalent-circuit model at various potentials with the DMFC anode operating at 80 °C

Potential ($V\ DHE^{-1}$)	R_m ($\Omega\ cm^2$)	R_i ($\Omega\ cm^2$)	$CPE_{i\text{-}Q}$ ($F\ cm^{-2}$)	$CPE_{i\text{-}p}$	R_{ct} ($\Omega\ cm^2$)	L_{co} ($H\ cm^{-2}$)	$CPE_{dl\text{-}Q}$ ($F\ cm^{-2}$)	$CPE_{dl\text{-}p}$	R_c ($\Omega\ cm^2$)
0.3	0.677	0.798	0.239	0.986	0.574	4.320	0.289	0.617	2.434
0.4	0.668	0.753	0.216	0.985	0.514	2.521	0.272	0.618	1.597
0.5	0.658	0.725	0.152	0.990	0.534	0.622	0.258	0.627	0.319
0.6	0.649	0.454	0.115	0.983	0.567	0.256	0.248	0.617	0.063

perature increases, the methanol oxidation reaction becomes more pronounced. The amount of $CO_{(ads)}$ increases as this species cannot be effectively oxidized to CO_2 at a lower potential (e.g., 0.3 V DHE^{-1}); therefore, L_{co} exhibits a larger value. On the other hand, as the potential increases to a higher value, e.g., 0.6 V DHE^{-1}, the $CO_{(ads)}$ species is efficiently oxidized to CO_2, so the amount of $CO_{(ads)}$ decreases and the L_{co} exhibits a smaller value as shown in Tables 2–4. These features were also found in the previous study indicating that the proposed CPE-based equivalent circuit model is also perfectly applicable to the DMFC anode using a high-metal-content Pt-Ru/CNT catalyst. In general, the used noninvasive approach is very suitable for conducting these particular impedance experiments.

4.4. Overall assessment of DMFC incorporated with high-metal-content anode catalyst

Based on the above experimental findings and the results obtained previously, an assessment of the DMFC anode using two different metal-content catalysts was made. It is clear that a high-metal-content is more favorable in every aspect, including easiness in anode fabrication, catalyst layer thickness and compactness, ionic resistance and catalytic activity. Overall, the high-metal-content catalyst reduces the amount of the carbon support material, which, in turn, favors the easy fabrication of the electrode and the complete utilization of the catalyst. This fact indicates that the reaction occurs on the electrode/membrane interface with a two-dimensional, i.e., a thin layer, manner. The thick catalyst layer forming a three-dimensional reaction zone, on the other hand, results in poor cell performance even the same catalyst loading is applied. In other words, this thin-layer electrochemical reaction scheme defies the conventional large reaction zone approaches as commonly employed in chemical reactor designs.

The experimental and the impedance analysis results also indicated that the catalyst layer is still too thick and the catalyst may not be fully utilized. The fabrication of the DMFC anode still left much to be desired. Therefore, it is desirable that the anode catalyst Pt-Ru/CNT as well as the cathode catalyst Pt/CNT with high metal contents (>70 wt%) and lower catalyst loadings (<2 mg cm^{-2}) should be used in the future studies, aiming at much thinner catalyst layers and more confined electrode structures, so as to further improve the performance of the DMFC for practical applications.

5. Conclusions

The effects of metal content of the CNT-supported electrocatalyst on the DMFC anode fabrication and the cell performance have been investigated. It was found that a high-metal-content catalyst (i.e., 40 wt%Pt-20 wt%Ru/CNT) exhibits a thinner catalyst layer with a buckypaper-type texture and a better anode fabrication than its low-metal-content counterpart (i.e., 20 wt%Pt-10 wt%Ru/CNT). Based on the same catalyst loading of the anode using these two catalysts, the latter required much more Nafion® solution (ionomer) binder and resulted in a much thicker catalyst layer on the anode. The optimal Nafion® ionomer content in the catalyst layer of the anode was found to be about 63.2 wt%. Overall, the DMFC incorporated with the high-metal-content catalyst exhibited a much better performance. A power density of >100 mW cm^{-2} can be obtained at 80 °C. The electrochemical impedance spectroscopy also indicated that the anode incorporated with a high-metal-content catalyst exhibited a much lower resistance and the catalyst could be fully penetrated and utilized in the DMFC operations. This accounts for the better cell performances observed. The electrochemical impedance investigation satisfactorily explained the observed characteristics of the DMFC anode. The better DMFC anode fabrications can be obtained at lower catalyst loadings using catalysts with even higher metal contents.

Acknowledgements

The authors gratefully thank financial supports from National Science and Technology Program for Nanoscience and Nan-

otechnology, and Institute of Nuclear Energy Research (INER) of Taiwan for the performance of this work.

References

[1] R. Yang, X. Qiu, H. Zhang, J. Li, W. Zhu, Z. Wang, X. Huang, L. Chen, Carbon 43 (2005) 11–16.
[2] C.A. Bessel, K. Laubernds, N.M. Rodriguez, R.T.K. Baker, J. Phys. Chem. B 105 (2001) 1115–1118.
[3] J. Guo, G. Sun, Q. Wang, G. Wang, Z. Zhou, S. Tang, L. Jiang, B. Zhou, Q. Xin, Carbon 44 (2006) 152–157.
[4] E.S. Steigerwalt, G.A. Deluga, D.E. Cliffel, C.M. Lukehart, J. Phys. Chem. B 105 (2001) 8079–8101.
[5] E.S. Steigerwalt, G.A. Deluga, C.M. Lukehart, J. Phys. Chem. B 106 (2002) 760–766.
[6] T. Yoshitake, Y. Shimakawa, S. Kuroshima, H. Kimura, T. Icjihashi, Y. Kubo, D. Kasuya, K. Takahashi, F. Kokai, M. Yudasaka, S. Iijima, Physica B 323 (2002) 124–126.
[7] T. Hyeon, S. Han, Y. Sung, K. Park, Y. Kim, Angew. Chem. Int. Ed. 42 (2003) 4352–4356.
[8] K. Park, Y. Sung, S. Han, Y. Yun, T. Hyeon, J. Phys. Chem. B 108 (2004) 939–944.
[9] W. Li, C. Liang, W. Zhou, J. Qiu, H. Li, G. Sun, Q. Xin, Carbon 42 (2004) 436–439.
[10] M.Y. Wang, J.H. Chen, Z. Fan, H. Tang, G.H. Deng, D.L. He, Y.F. Kuang, Carbon 42 (2004) 3257–3260.
[11] W. Li, C. Liang, W. Zhou, J. Qiu, Z. Zhou, G. Sun, Q. Xin, J. Phys. Chem. B 107 (2003) 6292–6299.
[12] G.L. Che, B.B. Lakshmi, C.R. Martin, E.R. Fisher, Langmuir 15 (1999) 750–758.
[13] Z. Zhou, S. Wang, W. Zhou, G. Wang, L. Jiang, W. Li, S. Song, J. Liu, G. Sun, Q. Xin, Chem. Commun. (2003) 394–395.
[14] W. Chen, J. Zhao, J.Y. Lee, Z. Liu, Mater. Chem. Phys. 91 (2005) 124–129.
[15] Z. Liu, L.M. Gan, L. Hong, W. Chen, J.Y. Lee, J. Power Sources 139 (2005) 73–78.
[16] N. Rajalakshmi, H. Ryu, M.M. Shaijumon, S. Ramaprabhu, J. Power Sources 140 (2005) 250–257.
[17] L. Li, Y. Xing, J. Electrochem. Soc. 153 (2006) A1823–A1828.
[18] Y. Goto, Small Fuel Cells for Portable Applications, Small Fuel Cells 2006, Knowledge Foundation, Washington, DC, April 2006.
[19] N.-Y. Hsu, S.-C. Yen, K.-T. Jeng, C.-C. Chien, J. Power Sources 161 (2006) 232–239.
[20] A.L. Ocampo, M. Miranda-Hernández, J. Morgado, J.A. Montoya, P.J. Sebastian, J. Power Sources 160 (2006) 915–924.
[21] I.D. Raistrick, D.R. Franceschetti, J.R. Macdonald, in: E. Barsoukov, J.R. Macdonald (Eds.), Impedance Spectroscopy Theory, Experiment, and Applications, second ed., John Wiley & Sons, Hoboken, NJ, 2005, pp. 87–91.
[22] C.-C. Chien, K.-T. Jeng, Mater. Chem. Phys. 99 (2006) 80–87.
[23] K.-T. Jeng, C.-C. Chien, N.-Y. Hsu, S.-C. Yen, S.-D. Chiou, S.-H. Lin, W.-M. Huang, J. Power Sources 160 (2006) 97–104.
[24] S. Kulesza, P. Szroeder, J.K. Patyk, J. Szatkowski, M. Kozanecki, Carbon 44 (2006) 2178–2183.
[25] Z. Wang, Z. Liang, B. Wang, C. Zhang, L. Kramer, Compos. Part A 35 (2004) 1225–1232.
[26] Y.-H. Chu, Y.G. Shul, W.C. Choi, S.I. Woo, H.-S. Han, J. Power Sources 118 (2003) 334–341.